Influence of porous support structure and the possible presence of defects on FO membrane behaviour

Mattia Giagnorio[a], Begüm Tanis[a], Claus Hélix-Nielsen[a], Fynn Jerome Aschmoneit[b,*]

[a] *Department of Environmental & Resource Engineering, Technical University of Denmark, Kgs. Lyngby, Denmark*
[b] *Department of Mathematical Sciences, Aalborg University, Copenhagen, Denmark*

Abstract

In forward osmosis, defects on the selective active layer and changes in the porous structure of the support layer can be detrimental factors affecting the membrane performance. This study focuses on the impacts of (i) the possible presence of defects and (ii) the changes in pore structures on the water flux and membrane selectivity via computational fluid dynamics analyses. Results suggest that diffusion of the draw solute through the support layer, i.e. internal concentration polarization, can be strongly enhanced or reduced by widening or narrowing the shape of the pore, respectively, while no significant effect on water permeation can be associated with the change in draw solution cross-flow velocity or in the loss of draw solute during filtration. Interestingly, defects within the active layer may affect the water flux exponentially as function of the defect size, suggesting the presence of a threshold below which the convective passage of contaminated water flux through the defect is not affecting the membrane productivity. Moreover, the presence of defects may not be a detrimental factor for membrane operating with high nominal rejection ($> 90\%$) and low percentage of defected area ($< 1\%$).

Keywords: Forward osmosis, defected area, pore support structure, ICP, pore shape geometry, cross-flow velocity, computational fluid dynamics, tortuosity

Nomenclature

AL	active layer
CFD	computational fluid dynamics
DM	defect model
DS	draw solution
ECP	external concentration polarization
FO	forward osmosis
ICP	internal concentration polarization
PM	porous model
PSS	porous support structure
TFC	thin film composite

*Corresponding author
Email address: fynnja@math.auu.dk (Fynn Jerome Aschmoneit)

1. Introduction

Membrane separation is an environment friendly, simple, and easily operated application process in water and wastewater treatment operations [1]. Considering the fact that the demand for clean and irrigation water are gradually increasing while 1.2 million people currently have limited access to clean and fresh water sources [2], the membrane separation process gains extra importance thanks to its advantages in operation and affordability. To deal with the current problems and near-future challenges, forward osmosis (FO) is one of the promising membrane separation processes as it uses the osmosis, which is a natural phenomenon, as its main driving force; therefore, it has the advantages of energy-efficient and sustainable operation [3]. The recent developments in membrane manufacturing process extended the FO applications since FO membranes are expected to be stable in the feed solution [3] with an asymmetric structure that has a selective thin layer and a thick support layer [4]. However, changes in both selective thin layer and the support layer can negatively affect the FO performance. Defects are the most known and possible changes on the selective thin layer, which result in performance decrement during the FO membrane operation. As Louie et al. [5] and Albo et al. [6] stated, the mesoporous and/or microporous defects remarkably decrease the gas separation capabilities of membranes, which can be used in FO process, in the dry state. Up to now, there are no noteworthy efforts on the understanding of defects in the selective thin layer and the impact of support structure on the FO performance. Ali et al. [7] worked on FT-30-type RO membrane and proposed an "in-situ" plugging approach for minimizing defects in the membrane. In the proposed approach, the mesoporous defects, which occurred during the short reaction time at the interface (between the organic and aqueous phases), were plugged by newly polymers. The increase in i) reaction temperature, ii) reaction time, and iii) degree of membrane crosslinking were main ways to achieve in-situ plugging approach. Hereby, a crucial performance improvement was observed in the gas separation properties, which can also reflect the performance improvement potential of separation process in a liquid environment. In the following study of Ali et al. [8], the developed defect-free membrane achieved the maximum rejection of 99.6% for the separation process of sodium chloride while the maximum rejection was obtained with 99.0% for separating boron. Besides the "in-situ' plugging or similar approaches, the Loeb-Sourirajan process can create defect-free membranes for RO process in cellulose acetate or triacetate (CTA) membranes [9], but it is not very clear for polyamide (PA) membrane types [10]. Refs. [5, 6, 11] showed that the PA membranes have defects on the selective layer that decreases the separation performance. Duan et al. [10] investigated the impacts of membrane properties and hydraulic pressure on the FO performance and found that the PA-TFC membranes had defects on the selective layer and hence there were remarkable performance decrement compared to CTA and PEBAX-coated PA-TFC membranes. Peters et al. [12] also pointed out the fact that the active layer properties crucially affect the permeability and compaction; therefore, higher operating pressure conditions (e.g. FO membranes) have dominant impacts on the intrinsic properties of the membrane and may result in defects in porous medium. Binger et al. [13] focused on the relation between the power density and specific energy consumption and recovery. It is emphasized that the power density can be enhanced by improvements in membrane conditions that include the minimization of defects under high pressure environments; otherwise, the defects limit the energy recovery potential. Besides the defects in the active layer of the membrane, the porous structure of the support layer has also an impact of the separation performance. Tiraferri et al. [14] stated that the best performance of the FO membrane process was based on the optimum structural characteristics of the support layer, which depended on the solvent quality, dope polymer concentration, fabric layer wetting, and casting. Hereby, the maximum porosity and minimum concentration polarization were achieved. Ren et al. [15] used commercially available ultrafiltration membranes and investigated the impact of the support layer pore size on the filtration performance. Four different molecular weight cut-off values were analyzed; 10 kDa, 50 kDa, 100 kDa, and 500 kDa. It was found that the roughness of the active layer was affected by the support layer pore size; thus, high fluxes could be operated with rougher membranes. Tang and Ng [16, 17] highlighted that the FO membranes made by looser fiber resulted in less resistance and high water diffusion, which increased the separating performance in the FO process. Bendoy et al. [18] added silicene nanosheets into polysulfone (Psf) support layer and observed the impact of silicene nanosheet loading, varied between 0% wt and 1.0%, on the FO performance. It was inferred that the loading of 0.25 wt% silicene nanosheet (SN0.25) had a finger-

like pore structure and the highest porosity and permeability while the low loadings of silicene nanosheet had negligible impact on the FO process. With a similar motivation, Ndiaye et al. [19] prepared two different poly (vinylidene fluoride)/polyacrylonitrile (PVDF/PAN) membranes with the mean fiber diameters of 7545 nm and 894 nm, respectively; thus they had different support layer thickness and porosity values. Even though both membrane types achieved higher selectivity than the reference commercial membrane (CTA) in FO process, the membrane with smaller fiber diameter had a better selectivity performance as it provided higher degree of crosslinking of the active layer. Another FO performance improvement study was presented by Dai et al. [20]; a graphene oxide (GO)-doped membranes were prepared for FO processes and nano-scale water channels were formed in perpendicular to the GO-doped membrane surface. The results showed that GO doping enhanced the surface morphology with the optimum GO doping of 0.15% wt, while the formed nan-scale water channels decreased the resistance and increase the water diffusion; thereby, a remarkable flux improvement was observed. The above-mentioned studies implied the impacts of the defects in the active layer and the porous structure in the support layer on the FO performance. Although the provided outputs improved the FO performance, there are still research gaps to be filled in for enhancing the FO performance with better understanding of the defects and the porous structure in the active layer and the support layer, respectively. This study points out those points and presents a generic framework for analysis of defects and porous structures in the active and support layers with different shapes and areas by using computational fluid dynamics (CFD). Thereby, the CFD method is proposed as an engineering approach for designing and analysis of pore structures in future FO membrane processes. Following the generic framework, two main contributions are i) various defect areas in the active layer, and ii) six different pore structure in the support layer. Then, the water flux trends are generated based on the various defect areas and pore structures.

2. Methods

Two separate models, namely (i) Porous Model - PM and (ii) Defect Model - DM were developed and their schematic representations are illustrated in Figure 1 while a detailed overview including the CFD boundary conditions are reported in the Supporting Information.

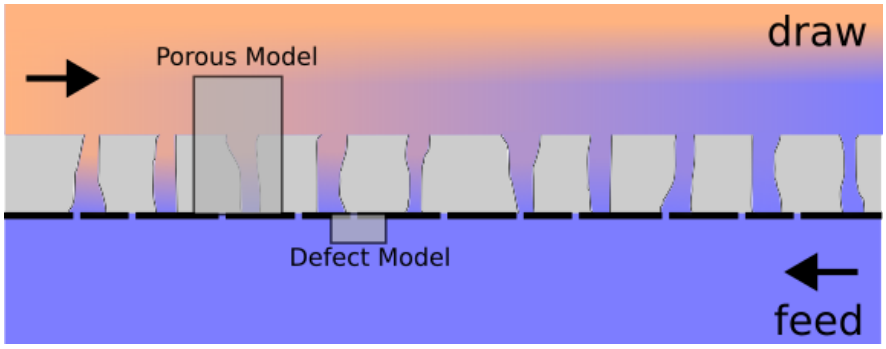

Figure 1: Schematic representation of the draw and feed channel with a porous support (grey) and an active layer (black) in a counter cross-flow setup. The draw solute gets diluted along the draw channel and inside the support pores (ICP). The two rectangles indicate the two models of this study: The Porous Model is used to investigate the influence of the porous support geometry, as well as the effect of (i) the reverse salt flux and (ii) the draw cross flow velocity on the ICP and the relative water flux through the AL. The Defect Model quantifies the potential contamination of the draw side ascribed to the convective passage of flow from the feed to the draw channel due to the presence of a defected Active Layer.

The PM was deployed to investigate the influence of the PSS geometry as well as the effect of (i) the reverse salt flux and (ii) the draw cross flow velocity on the internal concentration polarization (ICP) and the relative water flux through the AL. The model includes the TFC-FO membrane, designed as the combination of the membrane active layer (AL) and the porous support structure (PSS). The fluid dynamics of the draw solution (DS) was included in the PM by incorporating a section of the DS cross-flow channel while defining a parabolic profile to describe the relative cross-flow velocity. As described in next section and reported in

Fig3a, different porous geometries were investigated while fixing the operating boundary conditions of the PM. The DS was modeled as seawater, with an intrinsic NaCl concentration of 35 g/L and a representative bulk osmotic pressure of 28 bar. The diffusion coefficient of NaCl was included in the model as well as the its relative reverse salt flux B through the AL of the membrane (equal to 0.94 L $m^{-2}h^{-1}$). To model the water flux through the membrane an intrinsic permeability value A of 2.74 L $m^{-2}h^{-1}$ was taken into account. The choice of A and B was lab-based and obtained by testing an hand-made thin-film composite polyamide membrane during FO characterization experiments. Same values were used in previous studies to perform modelling analysis of forward osmosis systems [21, 22].

The DM includes a section of the cross-flow channel of the feed solution and only the relative AL of the TFC-FO membrane. With the goal of isolating and investigating the effects associated with the presence of defects within the AL, the draw side was intentionally not included in the model while the simulations were performed without considering the osmotic permeation through the AL, as this has no effect on the flow through the defects. The AL was modelled as a solid, impermeable wall, into which holes (defects) allow for local convective transport of feed flow. The CFD model thus models the flow in the feed channel in the direct vicinity of the AL, quantifying how much of the feed cross flow is convected into the defect, in dependence of cross-flow velocity and the defect size. Furthermore, with the goal of identifying a model describing the pure convective flow through the defected AL, simulations were performed considering pure water flowing within the feed channel, without accounting for potential contaminants dissolved in solution.

Based on the results obtained, a similarity relation for the convective passage of water from the feed to the draw site due to the presence of defects in the AL was derived. At a second stage, further simulations were developed adjusting the PM to include the similarity relation obtained through the DM with the goal of investigating effects of a defected AL on FO membrane behaviour, i.e., influence on ICP, the relative water flux and the potential changes in membrane selectivity due to contamination of the draw solution.

All CFD simulations were performed with OpenFoam v2012. As already reported in literature [23, 24, 25], this CFD tool is able to resolve the mass and momentum transfer across the geometries defined. The PM models the flow bu solving the incompressible Navier-Stokes equations, while the solute transport is modelled by the convection-diffusion equation. The solute density is not a function of the concentration but constant. Therefore, the bulk flow is affected by the local solute concentration. However, the boundary condition at the AL acts a flow inlet, in dependence of the solute concentration directly at the AL. The DM only considers flow; a solute concentration is not modelled. The flow field is not affected by the solute distribution

3. Results

3.1. Understanding the influence of different PSS and DS parameters on the resulting FO water flux

Influence of different pore shapes. The CFD simulations were performed on fundamental pore geometries, which are tailored to investigate the aspects of tortuosity and varying cross sectional areas. A schematic representation of the curved pore geometry is reported in Fig. 2a. An overview of all fundamental pore geometries is found in Fig. 3a. The straight pore channel (□) is used as reference to investigate the effect of pore shape variations on the ICP development. The overall results of these CFD simulations are reported in Fig.3. As expected, the results suggest that a geometrical variation of the porous support may strongly affect the resulting water flux through the active layer by influencing the diffusion of the draw solutes through the pores. This is visible in Fig.3b and d, showing the ICP profile within the porous support and the resulting water flux, respectively. In Fig.3b, the x axis is reporting the distance from the AL (x = 0) with an overall thickness of the pore equal to 150 μm.

Interestingly, a slight variation of the ICP profile was observed comparing the porous curve shape (▽ in Fig.3) to the a straight channel (□ in Fig.3). This variation can be ascribed to the difference in tortuosity between the two shapes. This result suggest that, in the presence of a fabricated membrane with a porous curve support structure characterized by a fixed (i) porous support thickness and (ii) homogeneous pore diameter, the actual water flux may be compared with the simulated water flux through an ideal membrane with straight pore channels, thus deriving the tortuosity and hence the structural parameter of the fabricated membrane. On the other hand, opening or reducing the internal pore section induce a less or more pronounced

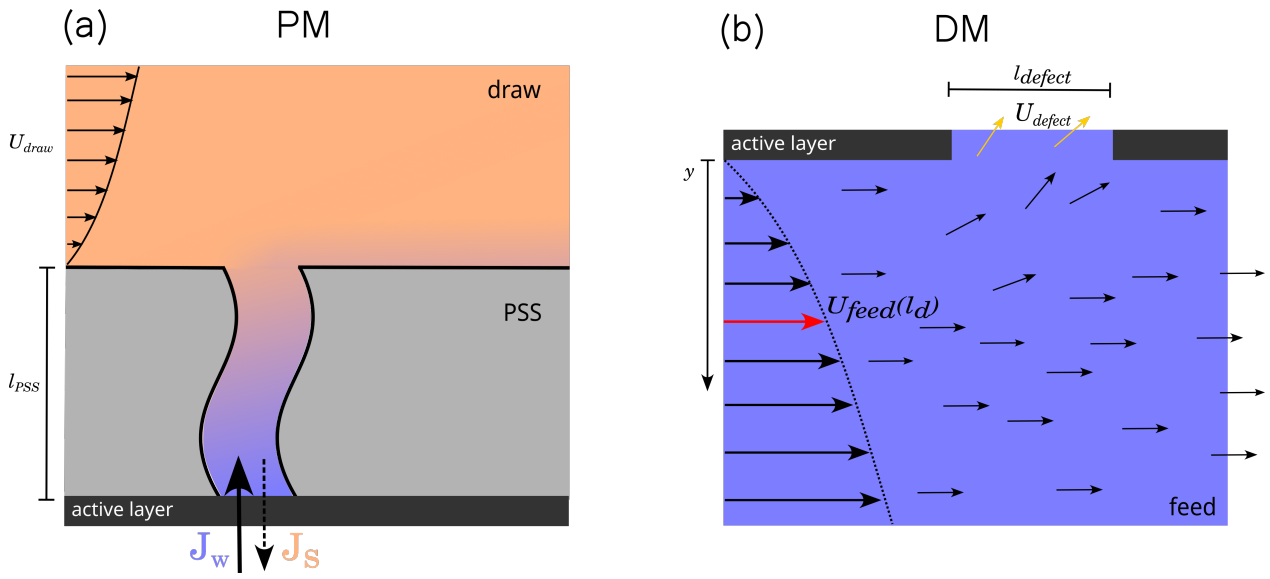

Figure 2: a) Porous Model represented by a single pore geometry. Blue and orange arrows represent the water and the reverse salt fluxes through the AL, respectively. The figure is reporting the curved shape, indicated with ▽ within the text. Alternative shapes were investigated and indicated as follows: straight □, narrowing cone △, widening cone ◇, concave cone ◯ and convex cone ⬠. b) Resolution of the Defect Model in the vicinity of the defect in the AL. The arrows indicate the local cross flow of water within the feed channel and the convective flow through the defect. resolution poor.a small part of the membrane vicinity, indicating local cross flow and flow through a defect in the active layer.

ICP profile (◯ and ⬠ in Fig.3), with a consequent increase or decrease of the resulting water flux through the AL, respectively (Fig.3d). However, the larger influence on FO membrane behaviour was observed by performing the CFD simulations while narrowing or widening the shape of the pore channel (△ and ◇ in Fig.3). In comparison with the straight pore case, the diffusion of the draw solute can be strongly enhanced or reduced by widening or narrowing the shape of the pore, respectively. A wider pore can induce a two times higher water flux occurring at the AL, compared to the equivalent narrower pore structure (Fig.3d). This is ascribed to the difference osmotic pressure resulting at the AL-draw solution interface and it may be explained considering that a large opening section at the porous-DS channel interface would increase the solute mass transfer, counterbalanced through an increase of the water flux through the AL at the steady state.

Influence of DS parameters: cross-flow velocity and reverse salt flux. Cross-flow velocity and reverse salt flux may be considered as the main DS parameters potentially affecting the FO membrane permeation. While the cross-flow velocity is an operating parameter of the FO filtration, the reverse salt flux strongly depends upon the choice of the draw solute. For instance, it is well known that the reverse salt flux through the same thin-film composite (TFC) membrane can be strongly reduced by choosing inorganic salts composed of multivalent ions instead of deploying more diffusive monovalent compounds such as sodium and chloride [26, 27, 28]. Figure 3c and 3d show the effect of the DS cross-flow velocity and reverse salt flux on water flux through the membrane, respectively. To observe the effect of the reverse salt flux, NaCl was simulated as draw solute and used as boundary conditions in the CFD simulations. Unexpectedly, results suggest that a change in cross-flow velocity or the loss of NaCl ascribed to the reverse salt flux affects marginally the resulting water flux at the active layer. Interestingly, this is true for each of the pore shapes investigated, suggesting that (i) the reverse salt flux has no significant influence on ICP at the pore scale and that (ii) the driving force ascribed to the DS concentration gradient at the AL is mainly exerted through the diffusive motion of the solute within the porous support. In other words, no significant effects on water permeation through the AL can be associated with the convective motion induced by the change in the DS

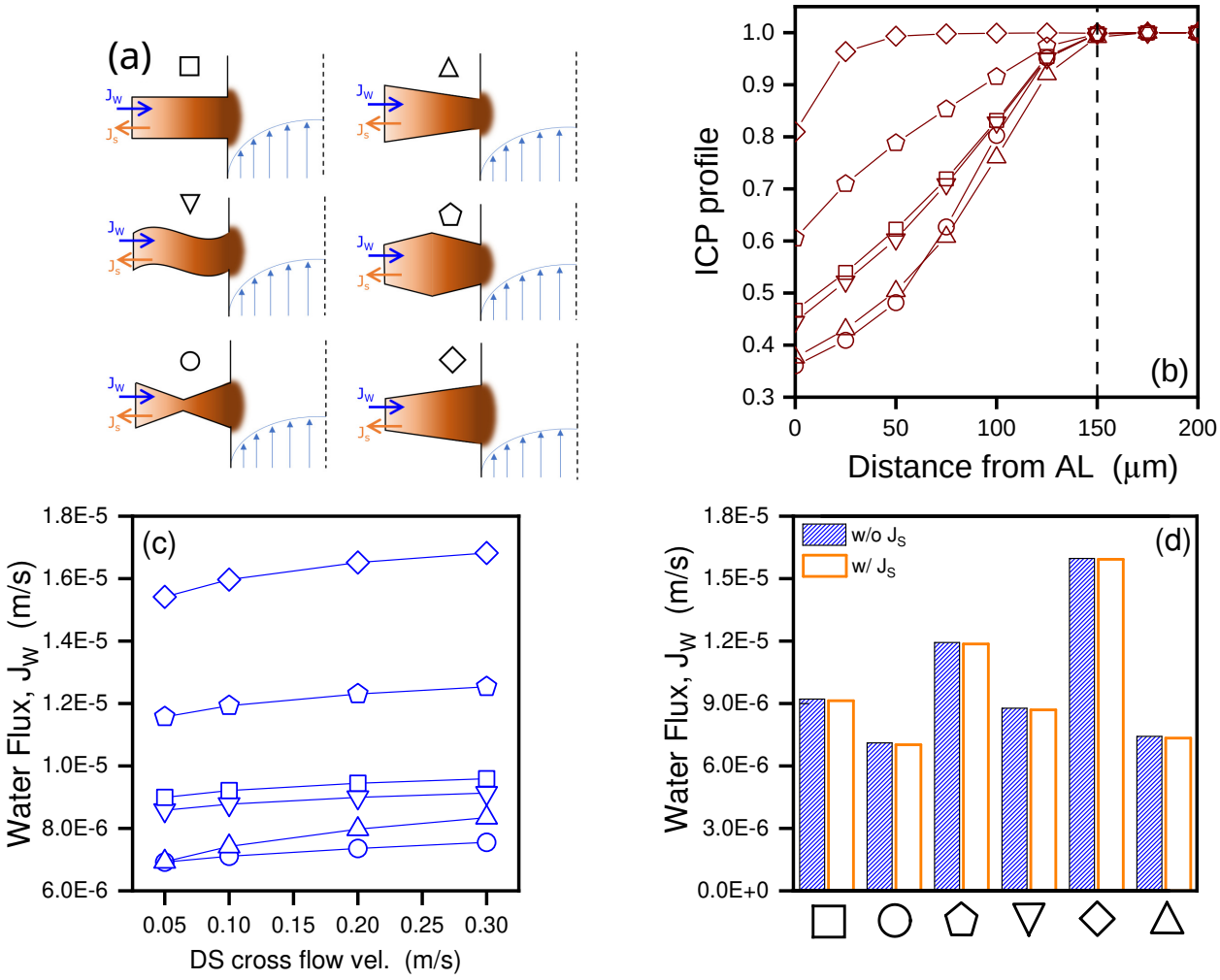

Figure 3: Influence of porous support structure and DS operating parameter on ICP and water flux in FO membrane. Investigation performed on a) different porous support geometries presenting the resulting b) ICP profile and c) water flux, the latter reported as function of the cross flow velocity variation. Influence of reverse salt flux B on water flux is presented in d) as function of the different porous support geometries.

cross-flow velocity or the loss of NaCl during filtration, regardless the type of pore shape characterizing the PSS. Overall, the results suggest that the DS cross flow velocity and the reverse salt flux of the draw solute does not represent critical parameters when designing new porous support structures for classical TFC FO membranes. However, it is worth noting that these parameters may affect the correct operation of the FO membrane, when placed in modules for real applications. For instance, depending on the membrane module configuration and operation (e.g., hollow fiber operated in counter-current) a significant variation of cross-flow velocity may be observed along the membrane area (both on the draw and feed side), potentially affecting the water recovery rate achieved [29]. On the other side, the reverse salt flux may represent a detrimental factor in real FO operation, such as in the Food and Beverage industry [30], responsible for the increase in the operational and environmental cost of the filtration system due potential contamination of the final products.

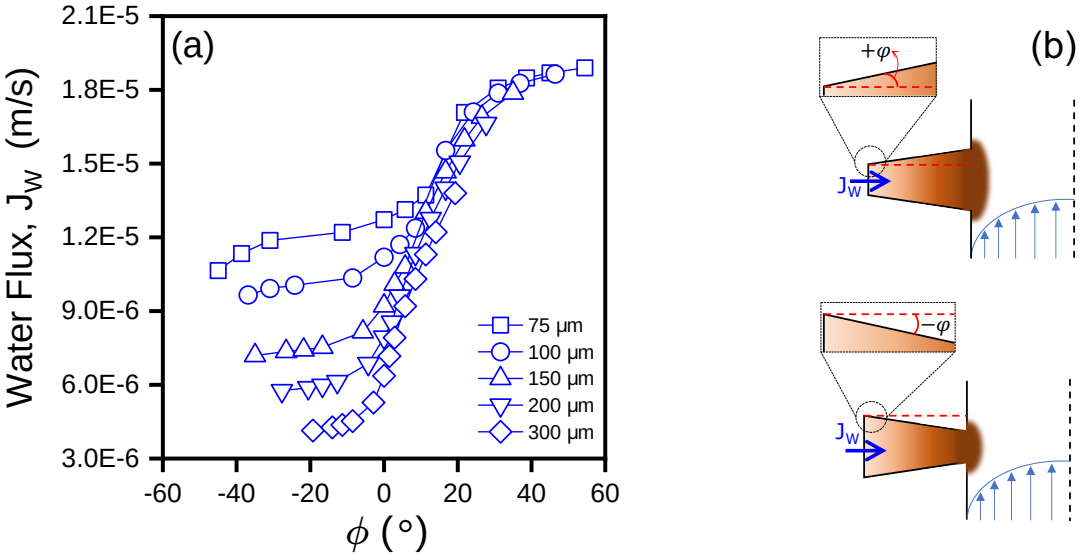

Figure 4: Influence of porous support (i) geometry and (ii) thickness on water flux through the membrane. Results of the CFD simulations are reported in a) showing the water flux J_W as function of a sensitivity analysis performed to investigate b) widening/narrowing conical pore geometries while varying the thickness of the porous support. □, ◯, △, ▽ and, ◇ refer to different porous support thicknesses and not to the pore shape as reported in previous figures

.

3.2. A more in-depth analysis of the PSS: influence of widening and narrowing conical pore shapes on the resulting FO water flux

Based on the results presented above, widening/narrowing the conical pore shape of the porous support is representing the geometrical factor, which most significantly affect the membrane permeability, i.e. geometries ◇ and △ in Fig. 3. To further investigate this effect, specific CFD simulations were performed through the PM by narrowing/widening simultaneously the conical pore in relation with the porous support thickness. The results of the simulations are reported in Fig.4. Each point in Fig.4a is representative of a CFD simulation, performed by changing (i) the thickness of the porous support (reported in the legend of the figure), as well as (ii) its narrowing/widening conical shape as described by Fig. 4b through the angle associated with the amplitude of the pore. Values for the porous thickness were chosen accordingly to what is reported in literature [31, 32, 33]. As expected, a lower thickness of the porous support entails an increase in the water flux through the membrane. This result is in accordance with what expressed in literature [34, 35]. Moreover, the structural parameter S is linearly proportional to the thickness of the support layer. Therefore, a lower support thickness would entail a decrease in the structural parameter, inducing larger water flux through the AL as reported in 4a. Practically, shortening the support thickness would reduce the ICP, ascribed to the reduction of the length of the pathway that the draw solute needs to be covered via diffusive motion prior to reach the AL. For this reason, during the last decades, research has been focused on new membrane materials and innovative fabrication procedures able to minimize the structural parameters of FO membranes [36, 37, 38, 39]. However, the results presented in Fig.4a suggest that a modification of porous support geometry towards a wider conical pore would strongly reduce the negative effect on FO membrane performances ascribed to a larger support thickness. The results indicate that similar water fluxes would be achieved by increasing the widening of the pore (φ positive) regardless the thickness of the support layer. On the other hand, to fabricate a more permeable FO membrane, a reduction of the porous support thickness is strongly suggested in the presence of narrower conical pores. These findings may have a substantial impact on future research development: new and high-performance FO membranes can be obtained by tailoring the shape of the porous support towards wider conical pores, without compromising on membrane thickness and mechanical stability fabricating thinner membranes. This would represent a great advantage in innovative

FO membrane application, such as in pressure retarded osmosis or pressure assisted forward osmosis, where the mechanical stability is an essential parameter for correct membrane operation. [40, 41].

3.3. Influence of defects in AL

The previous sections focused on fluid dynamics studies aim at understanding the influence of PSS and DS parameters on FO membrane behaviour, while simulating a perfect semi-permeable AL. However, AL may presents imperfections which can potentially affect the membrane filtration properties. To characterize the effects of the presence of defects within the AL in FO membranes operated in cross-flow filtration mode, the DM was developed. A schematic overview of the simulation is reported in Fig. 2b, where a defect (i.e., a hole) has been incorporated in the AL while reporting the local cross flow of water within the feed channel and the possible convective flow through the defect. The DM quantifies the defect velocity U_d as the mean velocity passing through the defect. To characterize U_d, we can derive the following assumptions and mathematical relations.

With reference to Fig. 2b, it is assumed that the feed velocity profile in the membrane vicinity is approximately parabolic. Specifically, the parabolic profile is a function of the bulk cross flow velocity $\mathbf{U}_f$ and the channel width w. The local cross flow at a specific distance y from the AL of the membrane can be defined as:

$$U_f(w,y) = \frac{3}{2}\mathbf{U_f}\frac{wy - y^2}{w^2} \tag{1}$$

Based on this feed flow profile, a series of simulations were performed through the DM by changing the defect lengths l_d in combination with the bulk cross flow velocity $\mathbf{U}_f$. The results are reported in Figure 5a. The data obtained from the simulations are represented as disks and crosses. The percentage of defected area is an indirect parameter referring to l_d , over a fixed length of the AL. Through the series of simulations described above , a similarity relation for the defect flow can be defined as follow:

$$\frac{U_d}{U_f(l_d)} = 1.77\left(\frac{l_d}{1\mu m}\right)^{\sqrt{2}} \tag{2}$$

Figure 5a plots the relative defect flow $U_d/U_f(w,l_d)$ against the absolute boundary flow $U_f(w,l_d)$, which relates to equation (1). For a given value of l_d, all data points lie on a horizontal line, i.e. the defect flow U_d is proportional to the bulk flow at distance l_d, $U_f(w,l_d)$. Furthermore, the results show that the data points are organized in constant plateaus, which only depend on the defect length l_d, i.e. the data seems to follow a scaling law. The entire data follows the scaling law in equation (2. The results show a good agreement between the simulations and the similarity relation, regardless the size of the boundary limits imposed in the simulations (i.e., the width of the cross-flow channel w). This suggests that a mathematical equation can be used to describe the imperfections of the AL when expressed as holes

Combining these two equations, and under the assumption of $l_d \ll w$, the defect flow can be expressed as a function of the bulk cross flow velocity and the defect width.

$$U_d\left(\mathbf{U_f}, l_d\right) \approx 2.66\mathbf{U_f}\frac{l_d}{w}\left(\frac{l_d}{1\mu m}\right)^{\sqrt{2}} \tag{3}$$

This is what reported in Figure 5b, where the defected flux (i.e., the convective water flow through the defect) is reported as function of the size of the defect incorporated in the AL (expressed as percentage of defected area). The graph is thus reporting a visual overview of what is expressed through eq. 2, showing that the defected flux is not only proportionally increasing with the size of the AL imperfection, but it is also exponentially affected by the increase of the cross-flow velocity applied within the feed channel. It is worth noting that the model does not include voluntarily the possible external concentration polarization (ECP) which may derive from the presence of dissolved species in the feed solution. The defected flux indeed would not be affected by ECP, since the water flow through the defect is driven by convective and not diffusive motion. However, dissolved or dispersed species in solution may be transported convectively through the AL imperfection, thus resulting in contamination of the draw solution.

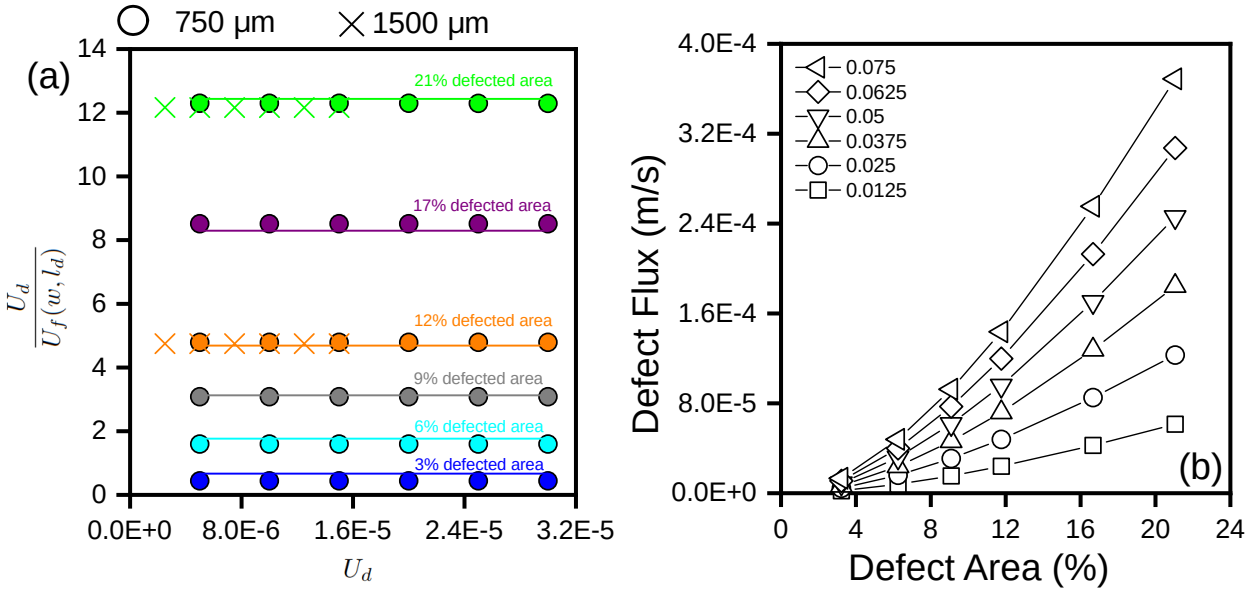

Figure 5: a) Relation of relative defect flow and near-wall cross flow and its dependence on the defect area. b) Defect flux against defect area: Defect flux is one order of magnitude greater than osmotic flux.

3.4. Understanding the influence of the defects within the AL in FO membrane performances

The output of the DM was incorporated in PM with the aim to investigate the effect of the presence of defects in the AL on ICP, water flux and membrane selectivity. The simulations were performed by modelling the straight pore channel, thus avoiding any coupling effect due to a different pore geometry. The results are reported in Figure 6. Figure 6a presents the water fluxes trends through the AL as function of the percentage of defected area, accounting for both the defected and total flux through the AL. While the defected flux is associated with the water leakage from the feed to the draw side due to the presence of defects, the total flux through the AL is considering both the defected flux and the water passage through the remaining intact section of the membrane via solution-diffusion. The defected flux is almost linearly increasing with the increase of the percentage of defected area, as in agreement with what expressed by the DM and the derived defect flux equation (2). On the contrary, the total water flux shows an exponential trend with the increase of the percentage of defected area. Interestingly, no significant effect was observed on total water flux for a defected area $< 3\%$. This may be ascribed to the low fraction of feed water passing through the defected area, which is insufficient to affect the overall water flux. On the contrary, when the percentage of defected area is $> 3\%$, the convective water passage is responsible for a larger dilution factor of the draw solute within the pore support, thus affecting the ICP as described in Fig.6b with evident effects on the total water flux (Fig.6a).

The results presented above (Fig.3c) imply that the draw solute and water transport within the porous support of a FO membrane is mainly governed by diffusion, while no significant effect is associated with the convective transport of solute through the water from the DS bulk. The presence of defects in AL would potentially lead to a convective mass transport of water and contaminants from the feed to the draw site. Since this would potentially affect the membrane performances via a reduction of the real membrane selectivity, a sensitivity analysis was carried out to assess the membrane rejection in the case of the presence of defects in the AL. The well known equation for calculating the membrane rejection R (eq.4) was taken into account, where c_p is representing the concentration of the contaminant in the product water (i.e., in the draw solution in FO case) and c_f the bulk concentration of contaminant in the feed solution. Without loosing generality, we assume a 0% rejection to contaminant within the defected area while the nominal rejection was varied from 0 to 100% for AL, thus representing the possible variation of the selectivity against different

pollutants depending on the characteristics of the membrane involved. Pollutants were modelled as inorganic ions dissolved in water and mass balances of water and solutes were carried out at the AL-solutions interface, accounting for the water fluxes trends obtained from the CFD simulations (Fig.6a).

Results are reported in Fig.6b and c, where contour plots are deployed to show the effective selectivity of an FO membrane characterized by a nominal rejection (y axis) and a percentage of defected area.

$$R = 1 - \frac{c_p}{c_f} \tag{4}$$

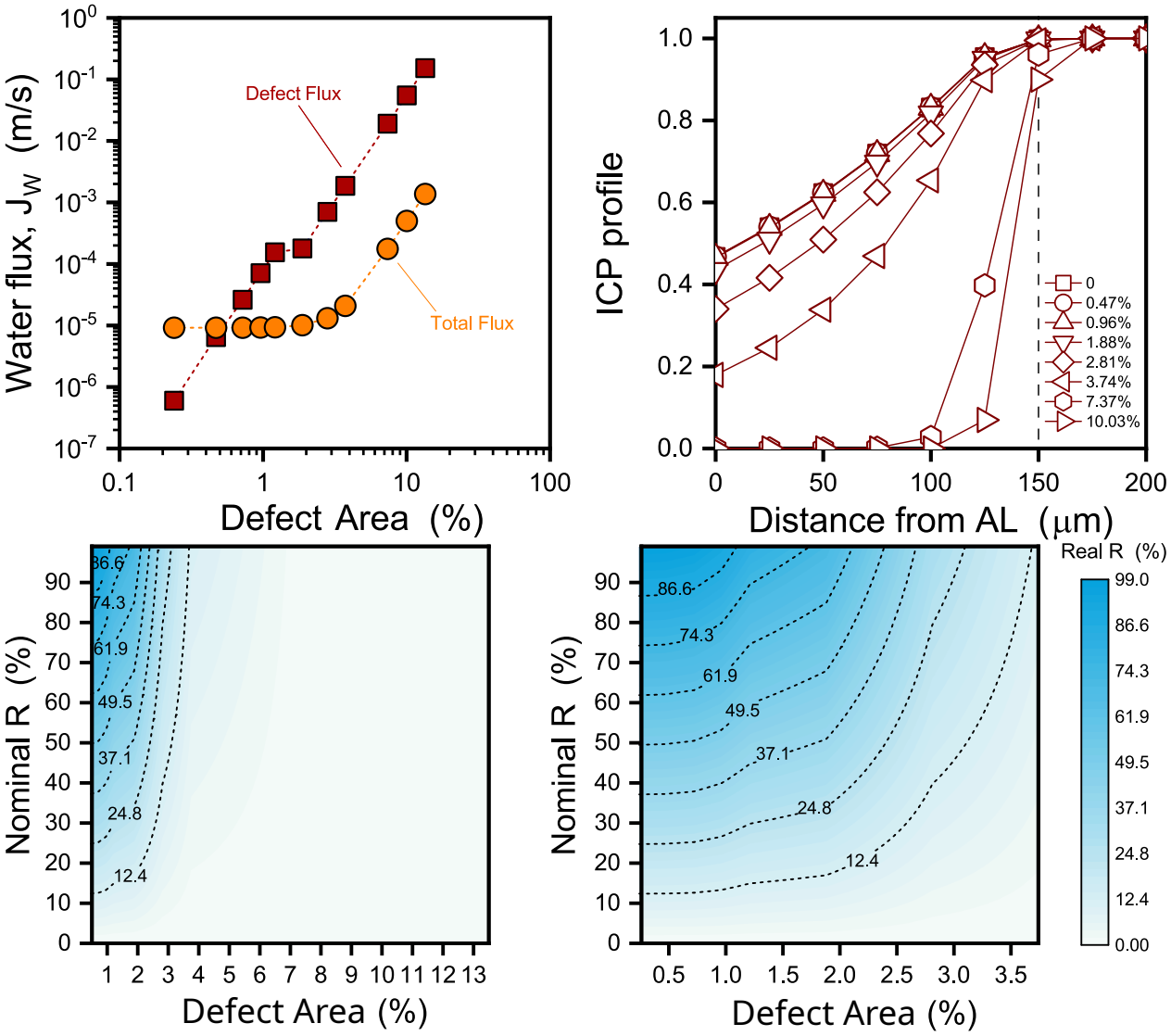

Figure 6: Influence of the presence of defects on the AL on membrane performances. Results present a) the water flux through the membrane as function of the increase of the defected area in AL. Water flux is distinguished between defected and total flux, thus incorporating both the convective flux through the defected area and the water passage through the AL, via solution-diffusion. The related ICP profile is reported in b), as function of the distance from the active layer. Counter-plots c) and d) report the real rejection of a TFC-FO membrane while varying its nominal selectivity (e.g., declared by the membrane manufacturer) as function of the possible presents of defects on the AL.

4. Conclusion & Outlook

This study reports a comprehensive modeling analysis of classical TFC membranes designed for Forward Osmosis applications (i.e., with the active layer facing the feed solution and the porous support structure facing the draw solution). Specifically, the study aims at understanding the influence of the pore support structure of the TFC membrane and the potential presence of defects within its active layer on water permeation and contaminants removal. An in-depth CFD analysis was performed by implementing two separate models in OpenFoam, namely Porous Model (PM) and Defect Model (DM).

The PM was used to investigate (i) the porous support structure and (ii) the draw solution operating parameters on membrane productivity. The CFD simulations were performed on fundamental pore geometries, tailored to investigate the aspects of tortuosity and varying cross sectional areas. Results suggest that a geometrical variation of the porous support structure may strongly affect the resulting water flux through the active layer by influencing the diffusion of the draw solutes through the pores. In particular:

- Opening or reducing the internal pore section induces a less or more pronounced ICP profile, with a consequent increase or decrease of the resulting water flux through the AL, respectively.
- Compared with a classical straight pore channel, the diffusion of the draw solute can be strongly enhanced or reduced by widening or narrowing the shape of the pore, respectively.
- A modification of the porous support geometry towards a wider conical pore would strongly reduce the negative effect on FO membrane performances ascribed to a larger support thickness, thus resulting in an increase of the water flux through the AL even in the presence of thicker membranes. This may potentially pave the way to future research development, aiming at developing suitable FO membranes for innovative applications, such as pressure retarded osmosis or pressure assisted forward osmosis where the mechanical stability of the membrane (i.e., membrane thickness) is a crucial parameter for correct operation.
- No significant effect on water permeation through the AL can be associated with the convective motion induced by the change in the DS cross-flow velocity or the loss of draw solute during filtration, regardless the type of pore shape characterizing the PSS. In other words, the DS cross flow velocity and the reverse salt flux of the draw solute does not represent critical parameters when designing pore support structures for new TFC membranes for FO applications. However, these parameters cannot be disregarded while instead, they may represent key parameters for scaling up promising FO membranes to pilot and real scale applications.

The DM was used to investigate the effect of the presence of defects within the AL in TFC membranes when operated in cross-flow mode. A new mathematical correlation was derived from the CFD results, where the defected flux (i.e., the convective water flow through the defected area) is reported as function of the size of the defect incorporated in the AL. Under the assumption of having the $l_d \ll w$ (defect length much smaller than the channel width) , the mathematical correlation is valid for any type of defects, regardless their geometry. The results suggest that the defected flux is not only proportionally increasing with the size of the AL imperfection, but it is also exponentially affected by the increase of the cross-flow velocity applied within the feed channel.

The model does not include the ECP. However, dissolved or dispersed species in solution may be transported convectively through the AL imperfection, thus resulting in contamination of the draw solution. To understand the effect of the presence of defects within the AL to the final membrane selectivity, the mathematical correlation developed was included in the PM for further CFD simulations. The resulting water flux through the membrane (accounting both the diffusive motion through the AL and the convective motion through the defected area) showed an exponential trend with the increase of the percentage of defected area, suggesting the presence of a threshold (3% of defected area) below which the convective passage of contaminated water flux through the defect is not affecting the membrane productivity. Finally, the sensitivity analysis performed to study the membrane selectivity resulting from the incorporation of defects within the

AL suggests, as expected, that the convective passage of contaminants from the feed to the draw side may strongly affect the quality of the water produced. However, the presence of defects may not be a detrimental factor for membrane operating with high nominal rejection ($> 90\%$) and low percentage of defected area ($< 1\%$), thus suggesting that even a non-perfect membrane can perform a valuable filtration when operated in cross-flow mode.

Acknowledgments

M.G., B.T., W.Z. and C.H.N. thank the Department of Environmental and Resource Engineering at the Technical University of Denmark. F.A. thanks the Department of Mathematical Sciences at Aalborg University, Denmark.

References

[1] G. Owen, M. Bandi, J. Howell, S. Churchouse, Economic assessment of membrane processes for water and waste water treatment, Journal of Membrane Science 102 (1995) 77–91, engineering of Membrane Processes II Environmental Applications.

[2] M. A. Shannon, P. W. Bohn, M. Elimelech, J. G. Georgiadis, B. J. Marĩas, A. M. Mayes, Science and technology for water purification in the coming decades, Nature 452 (7185) (2008) 301 – 310.

[3] L. A. Hoover, W. A. Phillip, A. Tiraferri, N. Y. Yip, M. Elimelech, Forward with osmosis: emerging applications for greater sustainability, Environmental science & technology 45 (23) (2011) 9824–9830.

[4] N. Widjojo, T.-S. Chung, M. Weber, C. Maletzko, V. Warzelhan, The role of sulphonated polymer and macrovoid-free structure in the support layer for thin-film composite (tfc) forward osmosis (fo) membranes, Journal of Membrane Science 383 (1) (2011) 214–223.

[5] J. S. Louie, I. Pinnau, M. Reinhard, Gas and liquid permeation properties of modified interfacial composite reverse osmosis membranes, Journal of Membrane Science 325 (2) (2008) 793–800.

[6] J. Albo, J. Wang, T. Tsuru, Gas transport properties of interfacially polymerized polyamide composite membranes under different pre-treatments and temperatures, Journal of Membrane Science 449 (2014) 109–118.

[7] Z. Ali, F. Pacheco, E. Litwiller, Y. Wang, Y. Han, I. Pinnau, Ultra-selective defect-free interfacially polymerized molecular sieve thin-film composite membranes for h2 purification, J. Mater. Chem. A 6 (2018) 30–35.

[8] Z. Ali, Y. Al Sunbul, F. Pacheco, W. Ogieglo, Y. Wang, G. Genduso, I. Pinnau, Defect-free highly selective polyamide thin-film composite membranes for desalination and boron removal, Journal of Membrane Science 578 (2019) 85–94.

[9] R. W. Baker, Membrane Technology and Applications (2nd edition), John Wiley & Sons, Ltd, Chichester, West Sussex, England, 2004.

[10] J. Duan, E. Litwiller, I. Pinnau, Solution-diffusion with defects model for pressure-assisted forward osmosis, Journal of Membrane Science 470 (2014) 323–333.

[11] P. Eriksson, Water and salt transport through two types of polyamide composite membranes, Journal of Membrane Science 36 (1988) 297–313.

[12] C. D. Peters, D. Y. F. Ng, N. P. Hankins, Q. She, A novel method for the accurate characterization of transport and structural parameters of deformable membranes utilized in pressure- and osmotically driven membrane processes, Journal of Membrane Science 638 (2021) 119720.

[13] Z. M. Binger, G. O'Toole, A. Achilli, Evidence of solution-diffusion-with-defects in an engineering-scale pressure retarded osmosis system, Journal of Membrane Science 625 (2021) 119135.

[14] A. Tiraferri, N. Y. Yip, W. A. Phillip, J. D. Schiffman, M. Elimelech, Relating performance of thin-film composite forward osmosis membranes to support layer formation and structure, Journal of Membrane Science 367 (1) (2011) 340–352.

[15] J. Ren, M. R. Chowdhury, J. Qi, L. Xia, B. D. Huey, J. R. McCutcheon, Relating osmotic performance of thin film composite hollow fiber membranes to support layer surface pore size, Journal of Membrane Science 540 (2017) 344–353.

[16] W. Tang, H. Y. Ng, Concentration of brine by forward osmosis: Performance and influence of membrane structure, Desalination 224 (1) (2008) 143–153, issues 1 and 2: 11th Aachener Membran Kolloquium, 28-29 March 2007, Aachen, Germany.

[17] H. Y. Ng, W. Tang, W. S. Wong, Performance of forward (direct) osmosis process: Membrane structure and transport phenomenon, Environmental Science & Technology 40 (7) (2006) 2408–2413.

[18] A. P. Bendoy, H. G. Zeweldi, M. J. Park, H. K. Shon, H. Kim, W.-J. Chung, G. M. Nisola, Silicene nanosheets as support fillers for thin film composite forward osmosis membranes, Desalination 536 (2022) 115817.

[19] I. Ndiaye, I. Chaoui, J. Eddouibi, S. Vaudreuil, T. Bounahmidi, Synthesis of poly (vinylidene fluoride)/polyacrylonitrile electrospun substrate-based thin-film composite membranes for desalination by forward osmosis process, Chemical Engineering and Processing - Process Intensification 181 (2022) 109132.

[20] C. Dai, D. Zhao, Y. Wang, R. Zhao, H. Wang, X. Wu, S. Liu, H. Zhu, J. Fu, M. Zhang, H. Ding, Impact of graphene oxide on properties and structure of thin-film composite forward osmosis membranes, Polymers 14 (18) (2022).

[21] M. Giagnorio, F. Ricceri, M. Tagliabue, L. Zaninetta, A. Tiraferri, Hybrid forward osmosis–nanofiltration for wastewater reuse: system design, Membranes 9 (5) (2019) 61.

[22] M. Giagnorio, A. Casasso, A. Tiraferri, Environmental sustainability of forward osmosis: The role of draw solute and its management, Environment International 152 (2021) 106498.

[23] F. J. Aschmoneit, C. Hélix-Nielsen, Computational fluid dynamics modeling of forward osmosis processes, in: A. Basile, A. Cassano, N. K. Rastogi (Eds.), Current Trends and Future Developments on (Bio-) Membranes, Elsevier, 2020, pp. 85–111.

[24] F. J. Aschmoneit, C. Hélix-Nielsen, Submerged-helical module design for pressure retarded osmosis:A conceptual study using computational fluid dynamics, Journal of Membrane Science 620 (2021) 118704.

[25] J. Ren, M. R. Chowdhury, L. Xia, C. Ma, G. M. Bollas, J. R. McCutcheon, A computational fluid dynamics model to predict performance of hollow fiber membrane modules in forward osmosis, Journal of Membrane Science 603 (2020) 117973.

[26] A. Achilli, T. Y. Cath, A. E. Childress, Selection of inorganic-based draw solutions for forward osmosis applications, Journal of membrane science 364 (1-2) (2010) 233–241.

[27] M. Giagnorio, F. Ricceri, A. Tiraferri, Desalination of brackish groundwater and reuse of wastewater by forward osmosis coupled with nanofiltration for draw solution recovery, Water research 153 (2019) 134–143.

[28] Q. Ge, M. Ling, T.-S. Chung, Draw solutions for forward osmosis processes: Developments, challenges, and prospects for the future, Journal of membrane science 442 (2013) 225–237.

[29] M. Giagnorio, M. Morciano, W. Zhang, C. Hélix-Nielsen, M. Fasano, A. Tiraferri, Coupling of forward osmosis with desalination technologies: System-scale analysis at the water-energy nexus, Desalination 543 (2022) 116083.

[30] G. Q. Chen, A. Artemi, J. Lee, S. L. Gras, S. E. Kentish, A pilot scale study on the concentration of milk and whey by forward osmosis, Separation and Purification Technology 215 (2019) 652–659.

[31] M. Kahrizi, R. R. Gonzales, L. Kong, H. Matsuyama, P. Lu, J. Lin, S. Zhao, Significant roles of substrate properties in forward osmosis membrane performance: A review, Desalination 528 (2022) 115615.

[32] N. D. Suzaimi, P. S. Goh, A. F. Ismail, S. C. Mamah, N. A. N. N. Malek, J. W. Lim, K. C. Wong, N. Hilal, Strategies in forward osmosis membrane substrate fabrication and modification: A review, Membranes 10 (11) (2020) 332.

[33] B. Kim, G. Gwak, S. Hong, Review on methodology for determining forward osmosis (fo) membrane characteristics: Water permeability (a), solute permeability (b), and structural parameter (s), Desalination 422 (2017) 5–16.

[34] J. R. McCutcheon, M. Elimelech, Modeling water flux in forward osmosis: implications for improved membrane design, AIChE journal 53 (7) (2007) 1736–1744.

[35] W. Li, Y. Gao, C. Y. Tang, Network modeling for studying the effect of support structure on internal concentration polarization during forward osmosis: Model development and theoretical analysis with fem, Journal of membrane science 379 (1-2) (2011) 307–321.

[36] M. Ghanbari, D. Emadzadeh, W. Lau, H. Riazi, D. Almasi, A. Ismail, Minimizing structural parameter of thin film composite forward osmosis membranes using polysulfone/halloysite nanotubes as membrane substrates, Desalination 377 (2016) 152–162.

[37] S. Zhang, K. Y. Wang, T.-S. Chung, H. Chen, Y. Jean, G. Amy, Well-constructed cellulose acetate membranes for forward osmosis: minimized internal concentration polarization with an ultra-thin selective layer, Journal of Membrane Science 360 (1-2) (2010) 522–535.

[38] Z. Zhou, Y. Hu, Q. Wang, B. Mi, Carbon nanotube-supported polyamide membrane with minimized internal concentration polarization for both aqueous and organic solvent forward osmosis process, Journal of Membrane Science 611 (2020) 118273.

[39] J. Baniasadi, S. Zarghami, F. S. Kamelian, T. Mohammadi, R. Nikbakht, Fabrication of asymmetric cellulose acetate/pluronic f-127 forward osmosis membrane: minimization of internal concentration polarization via control thickness and porosity, Polymer Bulletin 79 (1) (2022) 569–586.

[40] G. Blandin, A. R. Verliefde, C. Y. Tang, A. E. Childress, P. Le-Clech, Validation of assisted forward osmosis (afo) process: Impact of hydraulic pressure, Journal of membrane science 447 (2013) 1–11.

[41] A. Achilli, T. Y. Cath, A. E. Childress, Power generation with pressure retarded osmosis: An experimental and theoretical investigation, Journal of membrane science 343 (1-2) (2009) 42–52.